An Evaluation of Mass Flux Closures for Diurnal Cycles of Shallow Cumulus

R. A. J. NEGGERS,* A. P. SIEBESMA, AND G. LENDERINK

Royal Netherlands Meteorological Institute, De Bilt, Netherlands

A. A. M. HOLTSLAG

Department of Meteorology and Air Quality, Wageningen University, Wageningen, Netherlands

(Manuscript received 30 July 2002, in final form 1 March 2004)

ABSTRACT

Three closure methods for the mass flux at cloud base in shallow cumulus convection are critically examined for the difficult case of a diurnal cycle over land. The closure methods are first evaluated against large-eddy simulations (LESs) by diagnosing all parameters appearing in the closure equations during simulations of two different observed diurnal cycles of shallow cumulus. This reveals the characteristic behavior of each closure mechanism purely as a result of its core structure. With these results in hand the impact of each closure on the development of the cloudy boundary layer is then studied by its implementation in an offline single-column model of a regional atmospheric climate model. The LES results show that the boundary layer quasi-equilibrium closure typically overestimates the cloud-base mass flux after cloud onset, due to the neglect of significant moisture and temperature tendencies in the subcloud layer. The convective available potential energy (CAPE) adjustment closure is compromised by its limitation to compensating subsidence as the only CAPE breakdown mechanism and the use of a constant adjustment time scale. The closure method using the subcloud convective vertical velocity scale gives the best results, as it catches the time development of the cloud-base mass flux as diagnosed in LES.

1. Introduction

Mass flux models are widely used in convection schemes in operational general circulation models (GCM). The large-eddy simulation (LES) results of Siebesma and Cuijpers (1995) on the steady-state marine shallow cumulus case based on the Barbados Oceanographic and Meteorological Experiment (BOMEX; see Holland and Rasmusson 1973; Nitta and Esbensen 1974) show that the mass flux concept is capable of reproducing 80% of the vertical turbulent flux by the cumulus population. Although these results are encouraging, it is important to realize that many situations exist in which the boundary layer is far from steady state. A good example is a diurnal cycle associated with a cumulus-topped boundary layer over land, for example, as described by Brown et al. (2002) and Neggers et al. (2003). The strong variation of the surface heat fluxes during the daytime hours causes the boundary layer initially to grow in height by the heating of the mixed layer and by top entrainment in the inversion. The temperature and moisture of the mixed layer influence the onset of the clouds, as well as the height of the cloud base. These important parameters have been observed to fluctuate strongly during diurnal cycles of shallow cumulus (e.g., Neggers et al. 2003).

The non-steady-state nature of developing boundary layers potentially cause serious problems for mass flux schemes in single-column models (SCM). As shallow cumulus clouds are actually the visible part of (over)saturated thermals that root deeply in the subcloud mixed layer (LeMone and Pennell 1976), the subcloud and cloud layers strongly interact (Ogura and Cho 1974). Therefore it is necessary that in an SCM some coupling exists between the cumulus mass flux scheme and the subcloud mixed layer. This coupling is represented by the *closure* of the mass flux model at cloud base (Betts 1973, 1976), in which typically boundary layer parameters are used to estimate the cloud-base mass flux. Many different models for the mass flux closure have been formulated, often based on observations of marine steady-state cumulus fields. The question remains how the closures based on steady-state cases perform in the nonequilibrium case of a diurnal cycle over land. Possibly related to this issue are the reported prob-

* Current affiliation: Department of Atmospheric Sciences, University of California, Los Angeles, Los Angeles, California.

Corresponding author address: R. A. J. Neggers, Department of Atmospheric and Oceanic Sciences, University of California, Los Angeles, Los Angeles, CA 90095-1565.
E-mail: neggers@atmos.ucla.edu

© 2004 American Meteorological Society

Unauthenticated | Downloaded 05/30/24 05:45 AM UTC

lems of GCMs in dealing with the timing of precipitation and the triggering of deep convection over continental regions (e.g., Mace et al. 1998; Betts and Jakob 2002).

A range of mass flux closure methods exists, for both shallow and deep convection. Three well-known and often-applied closures will be studied in more detail. Based on budget studies of several field experiments (e.g., Augstein et al. 1973; Holland and Rasmusson 1973; Esbensen 1975), the mass flux model of Tiedtke (1989) explicitly assumes the subcloud mixed layer to be in steady state, which implies a constant moisture flux throughout the subcloud layer. Grant (2001) uses turbulent kinetic energy arguments to link the cloud-base mass flux to the convective vertical velocity scale of the mixed layer. In contrast to the previous methods, closures for deeper convection typically use characteristics of the cloud layer itself. Compared to shallow convection, deeper convection is driven by the relatively intense latent heat release in the convective clouds, which favors such an approach. One example is the Fritsch and Chappell (1980) closure, which associates the destruction of the convective available potential energy (CAPE) of the cloud layer with the compensating subsidence induced by the cumulus mass flux. Shallow cumulus often precedes deep cumulus on a convective day, and for parameterization purposes it is therefore important to know when the cloud layer is deep enough for this type of closure to work well.

This study follows the method of Siebesma and Holtslag (1996) of applying LES results in an SCM and to study their impact on the development of the boundary layer. First, the three mass flux closures mentioned earlier will be described in detail. Then the parameters which appear in the various closures will be sampled during LES simulations of diurnal cycles over land. This gives insight into the characteristics of each closure in such a situation. With these results in hand the closures are implemented in the convection scheme of Tiedtke (1989) as embedded in an offline SCM of the Regional Atmospheric Climate Model (RACMO; see, e.g., Lenderink and Siebesma 2000). In contrast to the LES runs where the closures are merely diagnosed, the closures then affect the vertical transport and hence the (thermo)dynamics of the developing boundary layer. The emphasis of this paper lies on determining the typical behavior of the resulting boundary layer as induced by the characteristic nature of each closure method.

The mass flux closures are described in section 2. The cumulus cases and the LES results are described in section 3. The RACMO SCM and its results are presented in section 4. Finally a discussion on the implications of the results and the conclusive remarks can be found in section 5.

2. Mass flux closures at cloud base

Applying the top-hat approach to the turbulent vertical flux of a variable ϕ conserved for moist adiabatic displacements results in the well-known mass flux equation (Ooyama 1971; Betts 1973),

$$\overline{w'\phi'} \approx M^c(\phi^c - \overline{\phi}), \tag{1}$$

where the mass flux M^c is defined as

$$M^c \equiv a^c w^c. \tag{2}$$

The parameter ϕ can be the liquid water potential temperature θ_l (Betts 1973) or total specific humidity q_t. Here, w is the vertical velocity, and the accent $'$ denotes a perturbation from the horizontal mean (denoted by the overbar). The superscript c stands for the horizontal average over the cloud core, defined as the fractional area a^c of the cloud ensemble which is both (over)saturated and positively buoyant. This fraction should be seen as the active cloudy part of the domain which is responsible for the bulk of the vertical turbulent transport (Siebesma and Cuijpers 1995). Equation (1) is the starting point of the mass flux model of Tiedtke (1989).

Observations and LES results have shown that the bulk mass flux of shallow cumulus cloud fields has its maximum at or very near cloud base (Esbensen 1978; Siebesma and Cuijpers 1995). In order to close the mass flux model, a closure at cloud base has to be formulated. We define cloud base here as the height at which the cloud (or core) fraction has its maximum. Three basic methods will be described in the next paragraphs. All the details of their subsequent implementation in the RACMO SCM are described in the appendix.

Note that this description of the various closure methods does not automatically imply that we also agree with them in all aspects: the prime purpose of this paper is to critically evaluate them, for which a detailed derivation is necessary. For a more thorough discussion and motivation of each closure we refer to the associated publications.

a. The moist static energy convergence closure

The first mass flux closure evolved from the outcome of a series of cumulus field experiments in the past that were situated in the oceanic trade wind region. Budget studies based on such datasets (Augstein et al. 1973; Holland and Rasmusson 1973; Ogura and Cho 1974; Esbensen 1975) have shown that the moisture tendency in the subcloud layer is typically negligible. This implies that the moisture flux at cloud base is equal to the moisture flux at the surface plus lateral advection at the sides of the domain (Kuo 1965, 1974; Tiedtke 1989). Applying (1) at cloud base and neglecting lateral advection at the sides for the moment then gives

$$M_b^c = \frac{(\overline{w'q_t'})_s}{(q_t^c - \overline{q_t})_b}, \tag{3}$$

where q_t is the total specific humidity. The subscript b indicates cloud base and s the surface. Similarly, the

Unauthenticated | Downloaded 05/30/24 05:45 AM UTC

moist static energy h can be used in this closure, which combines the heat and moisture fluxes,

$$M_b^c = \frac{(\overline{w'h'})_s}{(h^c - \overline{h})_b}, \tag{4}$$

where

$$h = c_p T + gz + Lq_v, \quad \text{and} \tag{5}$$

$$(\overline{w'h'})_s = c_p(\overline{w'\theta'})_s + L(\overline{w'q'_t})_s. \tag{6}$$

Here q_v is the water vapor specific humidity, T the temperature, g the gravitational acceleration, and z the height above the surface. The constant c_p is the specific heat of dry air at constant pressure and L is the specific latent heat of the phase change between water vapor and liquid water. When accounting for the large-scale advective and radiative tendencies $\mathrm{LS}_{\mathrm{adv}}$ and $\mathrm{F}_{\mathrm{rad}}$ in the subcloud layer Eq. (4) becomes

$$M_b^c(h^c - \overline{h})_b = \int_0^{z_b} \left(\mathrm{LS}_{\mathrm{adv}} + F_{\mathrm{rad}} - \frac{\partial \overline{w'h'}_{\mathrm{turb}}}{\partial z} \right) dz. \tag{7}$$

The dry turbulent flux divergence is included in order to properly connect the mass flux transport to the dry turbulence scheme at cloud base.

Closure (7) is used for shallow convection in the current version of the GCM of the European Centre for Medium-Range Weather Forecasts (ECMWF), as described in White (2001). This closure is also mentioned in the revision of the ECMWF convection scheme as presented by Gregory et al. (2000). Closure (7) will be referred to as the *moist static energy convergence* closure. Moist static energy has earlier been used for boundary layer closure purposes by Raymond (1995).

This closure method assumes that the rising, condensating thermals at cloud base, which are responsible for venting the heat and moisture into the cloud layer, are controlled by the quasi-equilibrium budget of moisture or moist static energy in the subcloud layer. The advantage of such an approach is that the mass flux at cloud base is directly linked to, among others, the surface fluxes, which are given parameters in a convection scheme. However, when part of the surface input of moisture and heat is deposited in the subcloud layer, the flux profiles decrease with height. Consequently the mass flux at cloud base will be overestimated by (7). A critical test is therefore its application to the nonequilibrium case of a diurnal cycle over land.

b. CAPE adjustment

In contrast to the boundary layer quasi-equilibrium closure, the adjustment closure is based on the assumption that the flux at cloud base is totally controlled by the conditions in the cloud layer. The quasi-equilibrium assumption states that any instability created by the slow-changing large-scale forcings is quickly destroyed by fast process of cumulus convection (e.g., Arakawa and Schubert 1974; Randall et al. 1997). Adjustment schemes associate a typical constant relaxation time scale with this process, relaxing the system towards a certain reference state (e.g., Manabe et al. 1965; Betts 1986; Betts and Miller 1986). For a more elaborate review of closures based on this method see for instance Emanuel (1994).

The reference state can be formulated in terms of the virtual potential temperature θ_v, which is also used in the definition of the convective available potential energy (CAPE),

$$\mathrm{CAPE} = \int_0^{z_i} \frac{g}{\Theta_v^0}(\theta_v^p - \overline{\theta_v})\, dz. \tag{8}$$

Here, Θ_v^0 is a reference value, and θ_v^p represents the profile of a dry/moist adiabatically rising element or parcel from the surface to its maximum height of ascent z_i, somewhere near or in the inversion. The parameter $\overline{\theta_v}$ is the horizontal mean. The adjustment principle using CAPE is expressed in terms of the relaxation formula

$$\left(\frac{\partial \mathrm{CAPE}}{\partial t}\right)_{\mathrm{conv}} = \frac{\mathrm{CAPE}}{\tau}, \tag{9}$$

where τ is the typical time scale associated with the adjustment process. It is the typical time scale of the conversion of the available potential energy into kinetic (convective) energy by the cloud ensemble. Arakawa and Schubert (1974) estimated the order of magnitude of τ at 10^3–10^4 s, based on the modeled scenario of the convective adjustment of a typical conditionally unstable cloud layer not maintained by large-scale forcings towards neutrality. When applied in GCMs the precise value of τ is commonly chosen somewhat freely. Nordeng (1994) suggested a time scale of 1 h, which is also used in this study. In the penetrative adjustment scheme of Betts and Miller (1986) a relaxation time scale of 2 h is used. For a discussion on this subject see Betts (1997).

The closure developed by Fritsch and Chappell (1980) links the adjustment of CAPE to the convective overturning induced by the cloud ensemble. Based on this approach is the closure proposed by Nordeng (1994) for deep convection in the ECMWF model, as described in White (2001) and also by Gregory et al. (2000). In this closure, the cloud ensemble is assumed to be in steady state (Tiedtke 1989) by which (8) can only change by modification of the $\overline{\theta_v}$ profile. The key assumption in the closure is that changes in $\overline{\theta_v}$ are dominated by the environmental subsidence as induced by the upward cumulus mass transport. The environmental tendencies due to convection can then be written as

$$\left(\frac{\partial \overline{\theta}}{\partial t}\right)_{\mathrm{conv}} \approx M^c \frac{\partial \overline{\theta}}{\partial z} \quad \text{and} \quad \left(\frac{\partial \overline{q_t}}{\partial t}\right)_{\mathrm{conv}} \approx M^c \frac{\partial \overline{q_t}}{\partial z}. \tag{10}$$

The tendency of CAPE in (9) can then be written as

Unauthenticated | Downloaded 05/30/24 05:45 AM UTC

$$\left(\frac{\partial \mathrm{CAPE}}{\partial t}\right)_{\mathrm{conv}} \approx -M_b^c \int_0^{z_i} \frac{mg}{\Theta_v^0} \frac{\partial \overline{\theta_v}}{\partial z}\, dz, \qquad (11)$$

where m is a normalized mass flux profile,

$$m(z) = \frac{M^c(z)}{M_b^c}. \qquad (12)$$

In combination with (9) this results in M_b^c as a function of CAPE and the $\overline{\theta_v}$ profile,

$$M_b^c = \frac{\mathrm{CAPE}}{\tau}\left(\int_0^{z_i} \frac{mg}{\Theta_v^0} \frac{\partial \overline{\theta_v}}{\partial z}\, dz\right)^{-1}. \qquad (13)$$

For application of this closure in the RACMO SCM a linear increase of M^c with height to its cloud-base value is assumed in the subcloud layer to ensure (i) conservation of mass and (ii) a smooth coupling with the dry turbulence scheme. For more details about the actual implementation in the SCM see the appendix.

By assuming a typical constant adjustment time scale the rhs of (9) becomes in fact a tendency that is imposed on the system. The rhs of (11) is the tendency that is possible by compensating subsidence, given the environmental lapse rate of θ_v. By normalizing the mass flux profile with the cloud-base mass flux, the latter becomes the only free parameter in the equation. Accordingly, the CAPE adjustment closure gives the mass flux at cloud base, which is needed to break down the existing CAPE entirely in time τ by compensating subsidence alone, given the environmental profiles as they are.

Several caveats are associated with this closure. First, it is not clear if a constant adjustment time scale is realistic. Second, in nonequilibrium situations such as a diurnal cycle the boundary layer is always in the process of reacting to cumulus convection in many ways. Apart from compensating subsidence CAPE is also affected by the detrainment of moist cloud air into the dry environment, by the deepening of the cloud layer by top entrainment of warm and dry inversion air, by forced convection, and also by moisture and temperature changes in the subcloud layer that affect θ_v^p. The cloud mass flux probably also plays a role in these processes, and leaving them out of (11) therefore gives a simplified closure relation.

The CAPE adjustment closure simply uses the mean convective instability present in the vertical column to set the intensity of the current mass flux transport at that time, through the process of compensating subsidence. This is just another way of saying that the relatively fast process of cumulus convection immediately adjusts to the instability that is created by the slowly changing large-scale forcings and is affected by earlier periods of convective activity (e.g., Arakawa and Schubert 1974; Randall et al. 1997). Limiting this interaction to the process of compensating subsidence alone is a simplification of reality.

c. Subcloud convective velocity scaling

A third method for mass flux closure relates the mass flux activity at cloud base to the turbulent kinetic energy (TKE) in the subcloud layer. This idea is based on observations that cumulus clouds often root deeply into the subcloud layer as dry thermals (LeMone and Pennell 1976). Accordingly, the kinetic energy and distribution of these condensated thermals at cloud base must bear the ''fingerprint'' of the dry turbulence convection in the subcloud layer. This links the physics of cumulus mass transport to subcloud-layer dry convection, which forms the conceptual basis for the third closure.

Following (2), the mass flux at cloud base is defined as the product of the core fraction and the core vertical velocity at that height,

$$M_b^c \equiv a_b^c w_b^c. \qquad (14)$$

The next step is to parameterize the two variables on the right-hand side using subcloud characteristics. By evaluating a budget equation for the TKE in the subcloud layer, Grant (2001) first scaled the cloud-base mass flux with the free convective vertical velocity scale of the subcloud layer w_{sub}^* (Deardorff 1970), defined as

$$w_{\mathrm{sub}}^* = \left(\frac{g z_b}{\Theta_v^0}(\overline{w'\theta_v'})_s\right)^{1/3}. \qquad (15)$$

Here, where z_b is the depth of the subcloud layer, θ_v is the average virtual potential temperature of the subcloud layer, and $(\overline{w'\theta_v'})_s$ is the buoyancy flux at the surface.

Our purpose is to relate w_b^c to a relevant convective velocity scale. The parameter w_{sub}^* only takes into account the vertical component of the TKE in the subcloud layer, while in high-shear situations the horizontal components may also contribute significantly. In those conditions some combination of w^* and u^* may be used in the definition of the subcloud turbulent velocity scale (e.g., Moeng and Sullivan 1994). Also, in deeper convective situations the relatively massive latent heat release in the clouds and the occurrence of precipitation may seriously affect the intensity of convection at and below cloud base, as is indicated by the occurrence of low-level gusts in the vicinity of deeper cumulus clouds. For those situations one could perhaps include some deep convective velocity scale in the parameterization for w_b^c, based on cloud-layer properties such as CAPE. This would represent a combination of the two different closure principles described before, the one controlled by the subcloud layer and the other by the cloud layer. Summarizing these options we write w_b^c as some function f of these three velocity scales,

$$w_b^c = f(w_{\mathrm{sub}}^*, u_{\mathrm{sub}}^*, w_{\mathrm{cloud}}^*). \qquad (16)$$

The central question of this study is how the various closures perform in a typical diurnal cycle of shallow cumulus, characterized by relatively low shear values and the absence of deep convection. Accordingly, here w_b^c will be scaled with w_{sub}^* only, and the other two op-

Unauthenticated | Downloaded 05/30/24 05:45 AM UTC

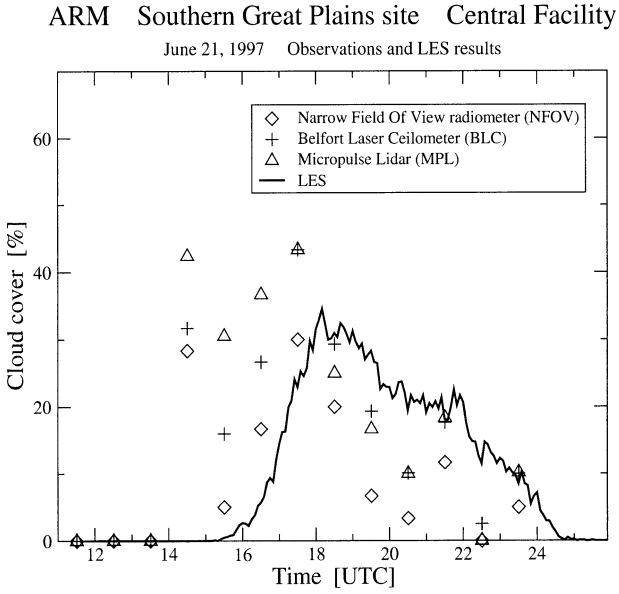

FIG. 1. Observations 21 Aug 1997 of the cloud cover at the ARM Southern Great Plains (SGP) site, Central Facility. Instrument measurements obtained from the ARM SGP Data Archive, which also provides extensive descriptions of these instruments. These are ceilometer-type instruments, measuring any cloud overhead and each using a different method. The LES results as discussed in the text are also shown. In a short period before cloud onset in LES some high cirrus clouds were observed at the SGP site, which might explain at least some of the early observations of cloud cover. Figure copied from Neggers (2002).

tions in (16) for deeper convection and more intense shear remain subjects for future studies. The scaling of w_b^c with w_{sub}^* will be evaluated using LES results on the diurnal cycle, during which w_{sub}^* varies considerably due to the changing surface buoyancy flux and cloud-base height.

By sampling the cloud-base mass flux and w_{sub}^* in LES for several different shallow cumulus cases Grant (2001) found the linear relation

$$M_b^c = 0.03\ w_{\text{sub}}^*. \tag{17}$$

Equation (17) suggests a relation between the cloud-base mass flux and the TKE budget of the subcloud layer. For a detailed derivation and a discussion on this subject we refer to Grant (2001). When comparing (14) to (17) it is tempting to see the factor of proportionality of 0.03 as a typical value for the core fraction at cloud base in shallow cumulus convection. However this is too ad hoc, as apart from the core fraction the factor represents many other assumptions and scaling factors.

Figure 1 shows measurements of the shaded cloud fraction at the Southern Great Plains (SGP) site of the Atmospheric Radiation Measurement (ARM) program (Stokes and Schwartz 1994). On this particular day a diurnal cycle of shallow cumulus was observed. It is evident that the cloud fraction changes significantly during the day. It might therefore be relevant to keep the nonconstant core fraction in formulation (14), instead of assuming it to be constant. This requires a parameterization for the core fraction at cloud base a_b^c, something yet to be developed. A possible solution for this problem in this study could be provided by LES results on other shallow cumulus cases (e.g., Brown et al. 2002; Siebesma et al. 2003). These studies suggest that the vertical profile of the core fraction a^c is always very similar to that of the cloud fraction a^{cl}, which in a SCM is commonly provided by a cloud parameterization scheme. This observation justifies the assumption that at least some relationship exists between these two parameters, which we describe by

$$a_b^c = \kappa a_b^{cl}, \tag{18}$$

where the variable κ defines the yet unknown relation. Equation (14) then becomes

$$M_b^c = \kappa a_b^{\text{cl}} \gamma w_{\text{sub}}^*, \tag{19}$$

where γ is a factor of proportionality between w_{sub}^* and w_b^c.

At this point the specific parameterization of κ and γ is left open, but LES results will be used later to study the typical behavior of these parameters during the diurnal cycle. The main reason for keeping the core fraction in (19) instead of a prescribed constant is that it introduces new first-order physical feedbacks in the single-column model that are realistic. First, the closure now knows when the dry subcloud-layer thermals reach their lifting condensation level. In practice, this means that in the SCM no mass flux transport can now occur without clouds (i.e., when the cloud fraction is zero). Second, a higher cloud fraction now leads to more intense mass flux transport, which (i) tends to decrease subcloud-layer moisture, which in turn decreases the cloud fraction, and (ii) results in more detrainment of moisture into the cloud layer, which also affects the cloud fraction. Accordingly, our main interest is not to exactly determine κ but to study the differences in impact of (17) and (19) as a result of these new first-order feedbacks. Therefore, both variations of this closure method will be evaluated.

3. Case descriptions and large-eddy simulations

a. Cases

In this section the cases representing the diurnal cycles are described. The first case is based on the development of shallow cumulus over land as observed on 21 June 1997 at the ARM SGP site. This case has been designed for an LES intercomparison study (Brown et al. 2002) by Working Group I of the GEWEX (Global Energy and Water Cycle Experiment) Cloud Systems Studies (GCSS; Browning 1993). Later the same case was used for model comparison studies as part of the European Project for Cloud Systems Studies (EUROCS). A diurnal cycle was observed in a cumulus-topped convective boundary layer over land. Radio-

Unauthenticated | Downloaded 05/30/24 05:45 AM UTC

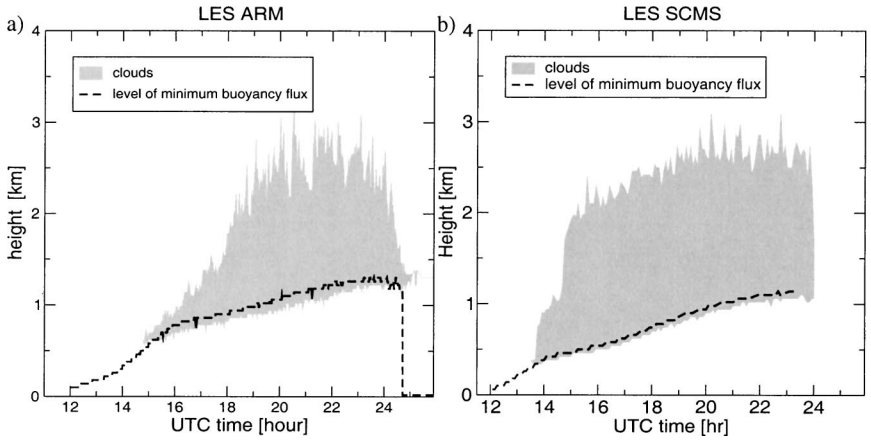

FIG. 2. The time series of the heights of cloud base and cloud top in LES for (a) the ARM case and (b) the SCMS case. The height of the minimum buoyancy flux is also shown to indicate the height of the mixed (subcloud) layer. Local time lags UTC time by 5 h in the SCMS case (FL) and by 6 h in the ARM case (OK).

sonde soundings, surface flux measurements, and cloud radar observations were made on this day. The surface heat fluxes make a full cycle from very low values at dawn to peak values at midday and back again. It is expected that this causes problems for many closures, as the mass flux at cloud base may consequently change in time. The ARM case is therefore a critical test case suitable for the purposes of this paper. The structure of the cloud layer of the ARM case in LES is plotted in Fig. 2a.

The second case also describes a diurnal cycle over land, as observed during the Small Cumulus Micro-Physics Study in August 1995 at Cocoa Beach, Florida (SCMS). An LES case was constructed based on radiosonde soundings, measurements of the surface energy balance, temperature, and moisture, and aircraft measurements inside the clouds (Neggers et al. 2003). Generally speaking this case closely resembles the ARM case, but there are some subtle differences. It is somewhat moister than the ARM case, featuring a relatively high cloud cover with a peak value of 41% shortly after cloud onset. The cloud layer in SCMS deepens relatively rapidly compared to the ARM case, due to the conditional instability already present at the heights where the clouds first develop (see Fig. 2b). Finally, the mean horizontal wind was much weaker in SCMS, which makes it a low wind shear case.

The basic characteristics and setup of these two cases are quite similar. Therefore, we focus the presentation of the results on the outcome of one particular case only. To this purpose we choose the ARM case, as it is at this moment the best known and most documented case of the two. In addition the SCMS case will primarily be used as a supplemental test ground for the closures, to evaluate the universality of the results on the ARM case at some vital points where the two cases differ.

LES is used to evaluate the performance of this range of closures in the two cases described earlier. The diurnal cycle is a critical test for these closures, as during the day the parameters on which the closures are based may change significantly. Time series of these parameters are derived by sampling the simulated cloud fields during the whole simulation. The performance of the resulting mass flux closures is evaluated by comparing the parameterized mass flux at cloud base with the actual value sampled in LES. This should immediately reveal the possible conceptual shortcomings of the closures. As the closures are designed to predict the mass flux of the active transporting updrafts in the cloud layer, we choose to compare the closures to the mass flux of the *cloud core* in LES.

b. Moist static energy convergence

Figure 3a shows the time series of the mass flux at cloud base as resulting from the boundary layer quasi-equilibrium closure and the CAPE closure. The moist static energy convergence closure (7) predicts too high values of the mass flux at cloud base during the first hours after cloud onset. Figure 4 offers a closer look into the moisture tendencies due to vertical transport in LES during the diurnal cycle. It is clear that in the period of overprediction of M_b^c the subcloud layer experiences ongoing moistening. It is evident that assuming the subcloud layer to be a constant moisture-flux layer does not hold in this period. A significant part of the surface input of moisture is deposited in the subcloud layer, and the subcloud layer also gets warmer in this period (e.g., Fig. 9c in the next section). Consequently the use of (7) overestimates the actual moist static energy flux at cloud base. As a result the mass flux at cloud base is overestimated. Later in the day the moisture-flux gradient in the subcloud layer in LES is much smaller, and consequently the moist static energy convergence closure performs better. The significant overestimation of the cloud-base mass flux by this closure in the early hours

Unauthenticated | Downloaded 05/30/24 05:45 AM UTC

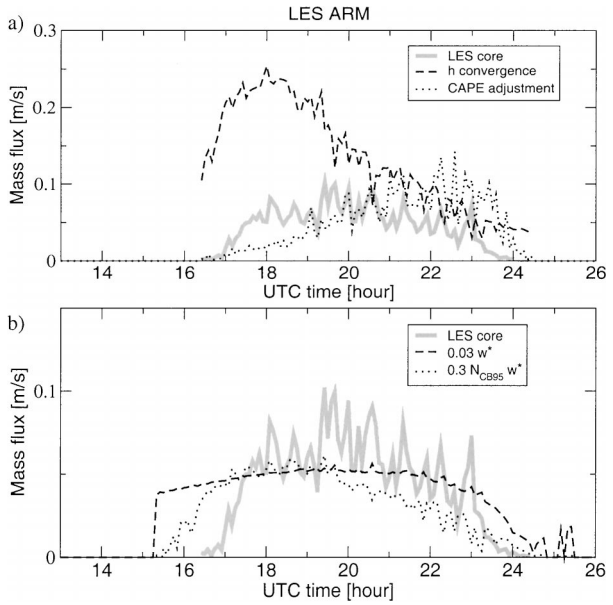

FIG. 3. The cloud-base mass flux in the ARM case as predicted by (a) the moist static energy convergence closure and the CAPE adjustment closure, and (b) the two versions of the w^* closure, based on parameters sampled during the LES run. The cloud-base value of the core mass flux in LES is plotted for reference.

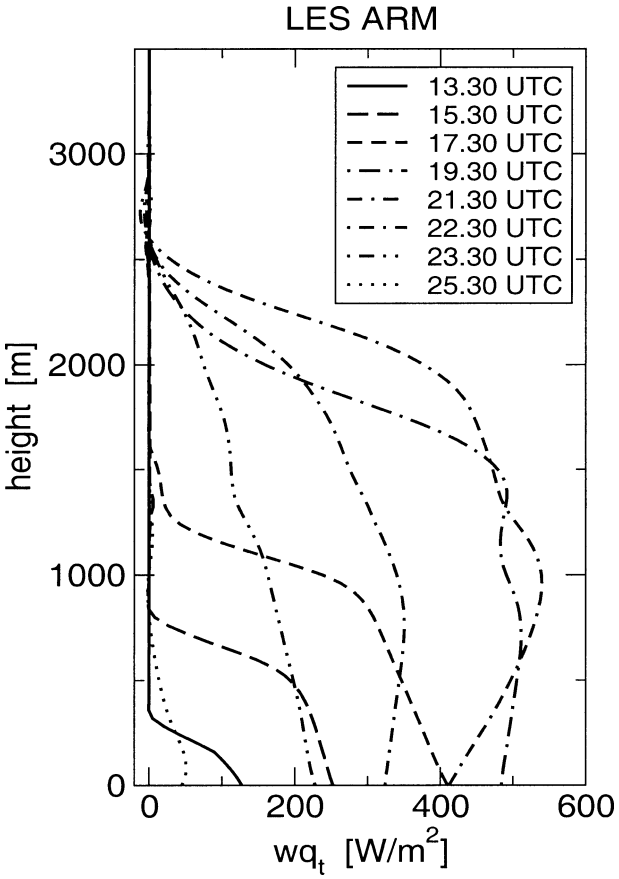

FIG. 4. Vertical profiles of the hourly averaged total moisture flux during the diurnal cycle of the ARM case in LES.

will cause too vigorous vertical transport into the cloud layer when applied in an SCM.

c. CAPE adjustment

Compared to LES, the CAPE adjustment closure gives the wrong trend for the cloud-base mass flux, with very small values in the early hours after cloud onset and relatively large values in the final hours, see Fig. 3a. To break down all existing CAPE in time τ by compensating subsidence a small (large) mass flux is apparently needed in the early (final) hours, but nevertheless the actual mass flux as diagnosed in LES is much larger (smaller).

As discussed earlier, two possible shortcomings might negatively affect the CAPE closure's performance, namely (i) the assumption of a constant adjustment time scale τ and (ii) the limitation of environmental subsidence as the only convective process that affects CAPE. Naturally, these features are related as more processes simultaneously destroying CAPE are collectively associated with a smaller adjustment time scale. The mispredicted trend in the mass flux at least implies that limiting convective CAPE destruction to compensating subsidence alone requires a variable time scale for this closure to work properly. Perhaps when including more processes acting on CAPE a constant adjustment time scale would be sufficient.

Figure 5 sheds some light on this problem during the course of the diurnal cycle, and gives some clues of what is actually happening. In the early hours after cloud onset CAPE is still very small. The cloud layer is also very shallow at this stage, see Fig. 2a. This suggests that the moist convection is of a forced nature, driven by subcloud-layer dry convection. As time progresses the CAPE closure gradually starts to overpredict the cloud-base mass flux, and the situation is reversed. Despite the large CAPE present at this stage the thermals which can become clouds are simply no longer ''triggered'' in the subcloud layer, due to decreasing surface heat fluxes that weaken subcloud-layer convection.

Summarizing, in the case of a diurnal cycle of shallow cumulus the dry convection in the subcloud layer controls the mass transport at cloud base in the early and final stages. The strict coupling of the cloud-base mass flux to CAPE via compensating subsidence alone in combination with a constant adjustment time scale is not sufficient for the closure method in such a developing coupled two-layer system, as it does not take the convection in the subcloud layer into account.

d. Convective velocity scaling

Closure method (19) still requires information on the variables κ and γ. Figure 6 shows that the cloud core

Unauthenticated | Downloaded 05/30/24 05:45 AM UTC

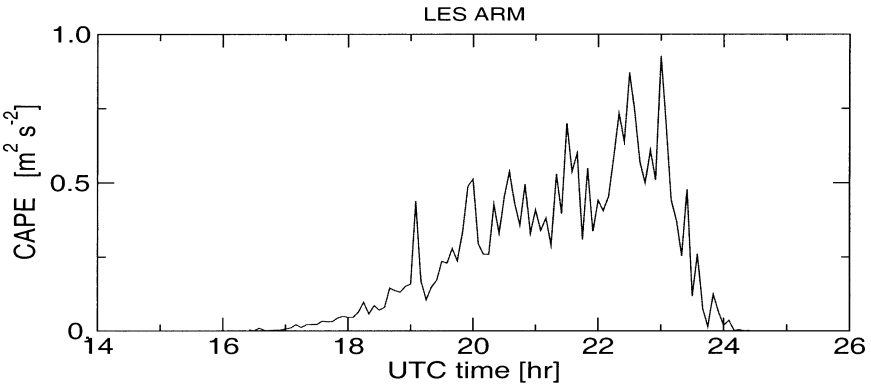

FIG. 5. The evolution of CAPE during the LES simulation of the ARM case. CAPE is in kinetic units, calculated using (8). Note that (11) is not a complete CAPE budget equation; it represents only the CAPE tendency by compensating subsidence. It should therefore not be seen as the actual change of CAPE with time as could be derived from this plot.

average vertical velocity at cloud base w_b^c as sampled in LES scales rather well with w^*_{sub}, especially in the SCMS case. Apparently the turbulence in the subcloud layer really does control the vertical velocity at cloud base. Based on these LES results we assumed a constant factor of proportionality $\gamma \approx 1$ in (19).

The cloud scheme in the RACMO SCM uses a statistical method to parameterize the cloud fraction a_b^{cl},

$$a_b^{\text{cl}} = N_{\text{CB95}}(z_b), \tag{20}$$

where the term N_{CB95} refers to the ''partial cloudiness'' N as proposed by Cuijpers and Bechtold (1995), for a more detailed description see the appendix. Figure 7 illustrates that similar to the LES cloud fraction at cloud base, N_{CB95} decreases with time, although it clearly underpredicts the maximum at 1800–1900 UTC.

For the sole purpose of exploring new feedbacks between core fraction and mass flux, choosing a constant factor of proportionality between cloud and core fraction $\kappa = 0.3$ in (19) is sufficient. This ensures that at least the first-order behavior of the core fraction is captured by closure (19), which is our main purpose. We again emphasize that by no means do we consider κ to be a universal constant; it is used for the single purpose of introducing the first-order feedbacks between core fraction and mass flux in the single-column model as opposed to them being absent. For a more general use of (19) a more sophisticated parameterization of the core fraction is needed.

Figure 3b shows that both versions of the w^* closure (19) and (17) predict cloud-base mass fluxes that are in phase with LES. The maximum mass flux occurs at the right time, and the collapse of the cloud mass flux at the end of the day is also captured. Apart from these promising characteristics, which are due to the use of w^*_{sub} shared by both versions, there are some differences. Figure 3b shows that (19) predicts a more gradual increase of the cloud-base mass flux in the early hours after cloud

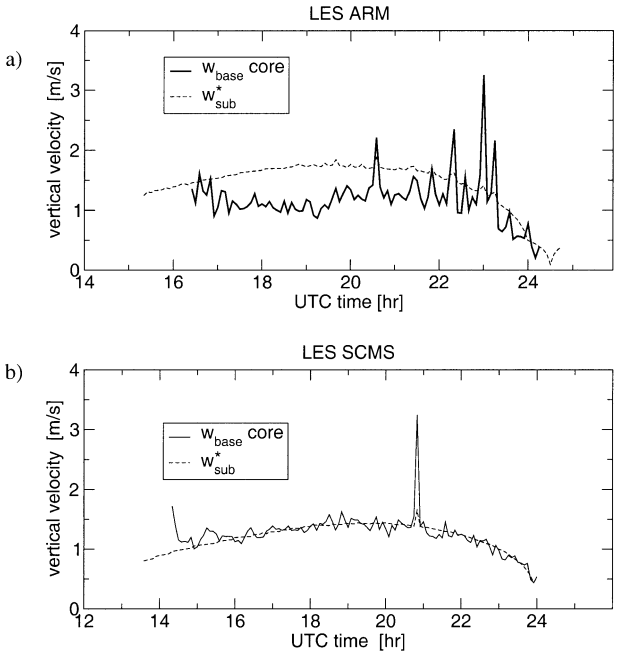

FIG. 6. The conditionally sampled vertical velocity of the cloud core at cloud base, and the convective vertical velocity scale of the subcloud layer (w^*_{sub}): (a) The ARM case and (b) the SCMS case.

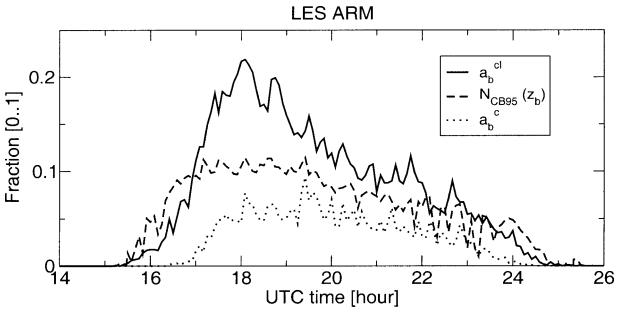

FIG. 7. The cloud and core fraction at cloud base in LES, and the parameterized cloud fraction N_{CB95} of Cuijpers and Bechtold (1995) also at cloud base [see (A1)].

Unauthenticated | Downloaded 05/30/24 05:45 AM UTC

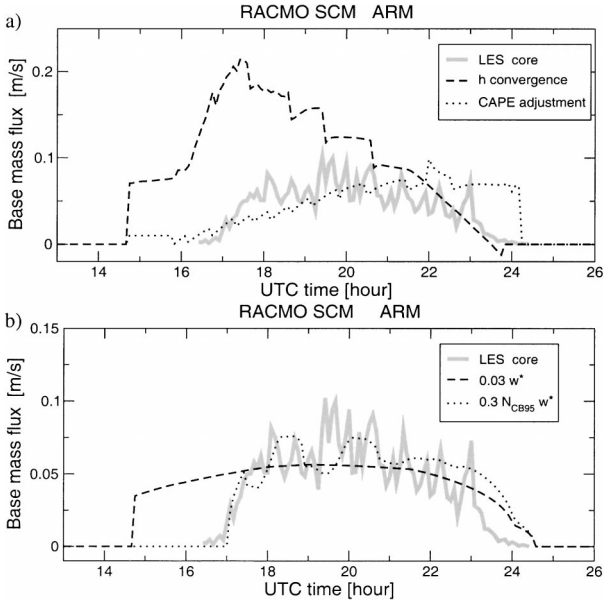

FIG. 8. The cloud-base mass flux in RACMO SCM as predicted by (a) the moist static energy convergence closure and the CAPE adjustment closure, and by (b) the two versions of the w^* closure. The cloud-base value of the core mass flux in LES is plotted for reference.

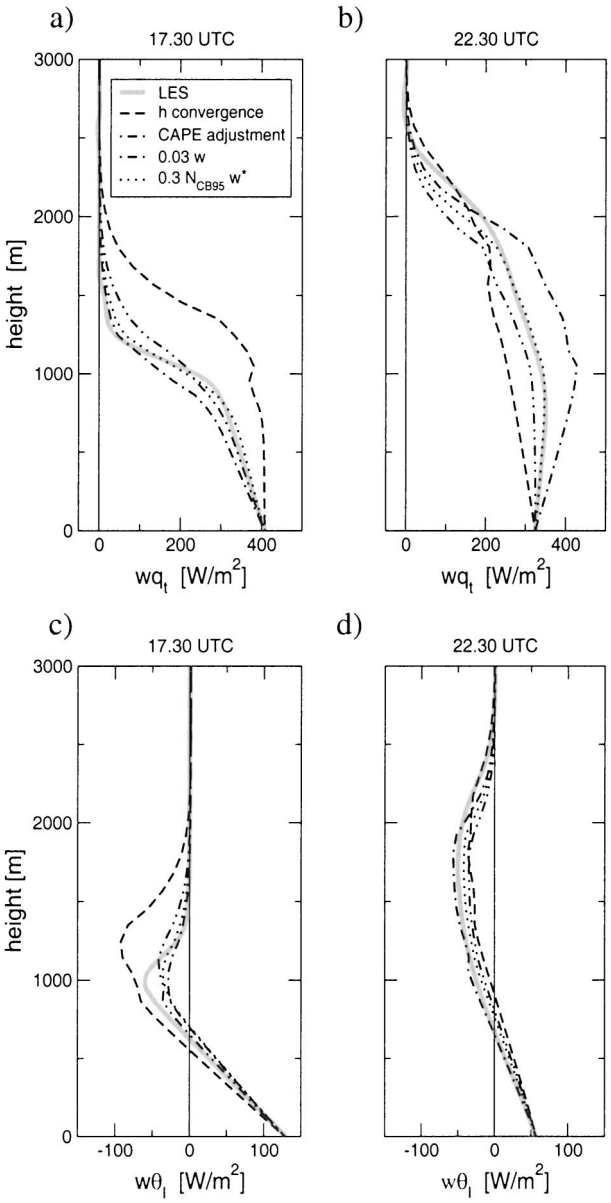

FIG. 9. The total moisture and heat fluxes of the ARM case in RACMO SCM at 1730 and 2230 UTC. The LES profiles are plotted for reference.

onset, which more closely resembles the LES timeseries. Also, after the maximum at 1900 UTC it decreases more or less linearly. These differences are due to the inclusion of the core fraction in (19). Equation (17) produces cloud-base mass fluxes too early due to the fact that it has no knowledge on whether or not active thermals are reaching their lifting condensation level.

4. Single-column model results

a. Description of the model

The three closures are implemented in the convection scheme of the offline RACMO single-column model (SCM). In the LES analysis described in the previous section the time series of M_b as predicted by the various closures are purely diagnostic: they show what the closures predict given the parameters as they are in LES at that moment. In contrast, implemented in the single-column model the closures affect the development of the (thermo) dynamic state of the boundary layer. The underlying physical causes for the typical behavior of the various closures are already analyzed and discussed in the previous section 3. This section focuses on how the development of the boundary layer in the SCM is affected differently by the various closures. The RACMO SCM and the implementation of the closures are described in detail in the appendix.

b. Results

Figure 8 shows the time series of the cloud-base mass flux during the ARM case in the RACMO SCM. Comparing these to Fig. 3 illustrates that in general the RACMO SCM results more or less resemble the corresponding diagnostic tests in LES.

The moist static energy convergence closure (7) predicts a cloud-base mass flux that is 3 times too large in the early hours. Figure 9 shows the corresponding flux profiles of heat and moisture at two moments in the diurnal cycle. At 1730 UTC the moist static energy convergence closure per definition predicts an almost constant moisture flux in the subcloud layer, while according to LES it should be moistening considerably. As a consequence most of the surface moisture flux is

Unauthenticated | Downloaded 05/30/24 05:45 AM UTC

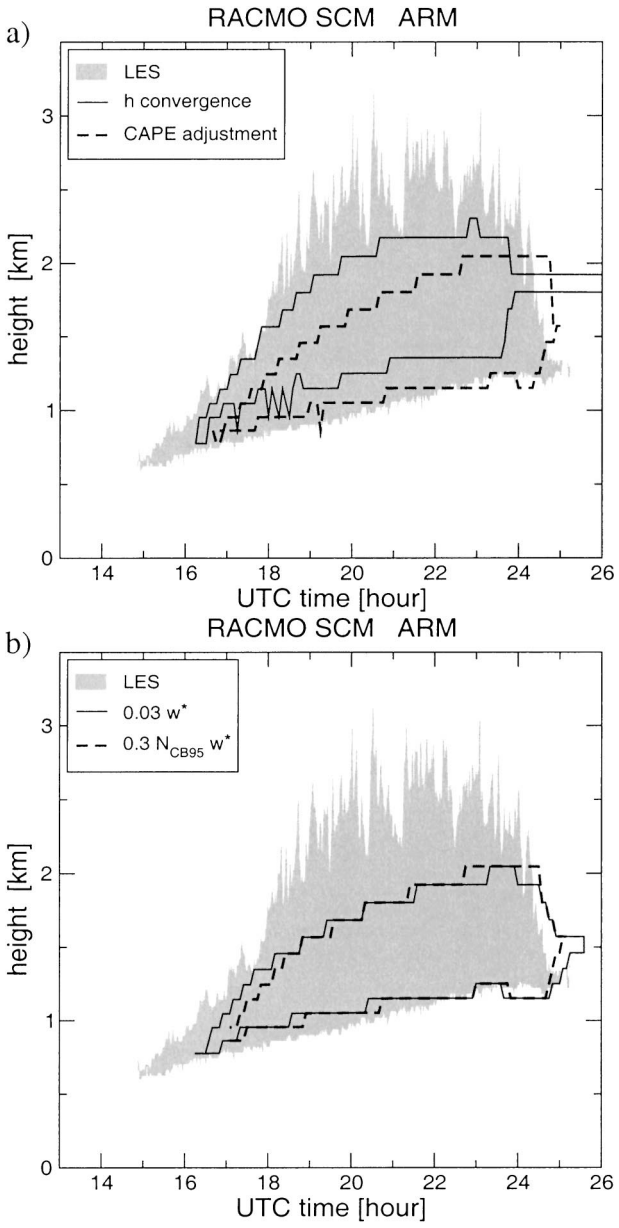

FIG. 10. The heights of cloud base and cloud top during the RACMO SCM simulations of the ARM case. The LES cloud heights are also plotted for reference. Note that the top-hat mass flux scheme in RACMO SCM is not designed to predict cumulus overshoots into the inversion, which appear as spikes in the cloud-top height in LES.

transported into the cloud layer and the inversion, where it causes a too rapidly deepening cloud layer, see Fig. 10a. The associated relatively intense vertical mixing in the inversion entrains more warm and dry air into the boundary layer, which as a whole heatens too rapidly compared to LES. This causes the cloud base to rise too fast, see Fig. 10a. At 2230 UTC when the cloud layer is fully developed the situation is reversed, as the heat and moisture fluxes at cloud base are now too small.

The application of the CAPE adjustment closure in

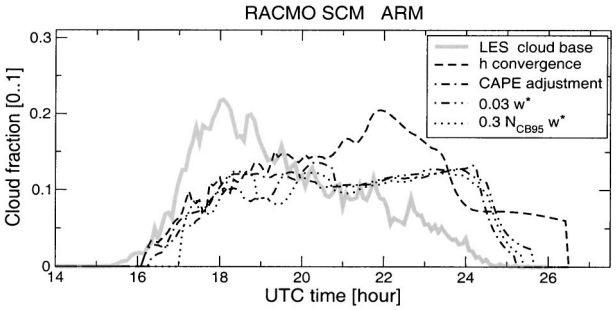

FIG. 11. The cloud fraction at cloud base during the RACMO SCM simulations. The LES time series is also plotted for reference.

RACMO SCM resembles its evaluation in LES, as the mass flux at cloud base shows the same (increasing) trend. Figure 8a illustrates that first M_b is too small, but as the CAPE increases with time so does M_b, and is significantly overpredicted in the final hours. Figure 9d shows that the resulting too large moisture flux at cloud base causes too intense drying in the subcloud layer. The rise of cloud base with time in LES is reproduced by RACMO using the CAPE closure, which results from the fact that the order of magnitude of the predicted mass flux at cloud base is comparable to LES. Apparently the adjustment time scale τ of 1 h is of the right order of magnitude in this situation.

Both versions of the ω^* closure predict the maximum cloud-base mass flux at approximately the right time, and also reproduce the collapse of mass flux transport at the end of the day, see Fig. 8b. The flux profiles in Figs. 9a and 9b show that this closure also reproduces the initial moistening and subsequent drying of the subcloud layer. The only problem with (17) occurs in the first 2 h, when the convection scheme is already active in RACMO SCM but the cloud scheme is not (i.e., the cloud fraction is still zero). The inclusion of the cloud fraction in (19) instead of assuming it constant prevents mass flux activity in the absence of clouds.

The sensitivity of the mass flux to the cloud fraction in (19) also becomes clear in the final hours, when M_b^c is slightly overestimated. This is caused by the cloud parameterization N_{CB95}, which does not predict the typical decrease with time here, see Fig. 11. Figure 7 shows that in principle N_{CB95} does predict a decreasing cloud fraction when fed with the right parameter values. Therefore, (A1) implies that the estimate of the saturation deficit variance does not develop correctly with time. Improving this remains a subject for further research.

5. Discussion and conclusions

We chose to examine the mass flux closure methods by first diagnosing each formulation in LES and subsequently by testing their impact on the developing boundary layer when embedded in an offline SCM. The use of this approach lies not in determining exact values

Unauthenticated | Downloaded 05/30/24 05:45 AM UTC

for factors or constants that might appear in a closure formulation. Its true use in the direct evaluation of closure ideas and concepts against LES with each mechanism stripped bare to the essential equations. This reveals the characteristic behavior of each closure mechanism purely as a result of their structure. It excludes any possible influence of other modules and parameterizations which accompany a closure parameterization when embedded in an SCM. The resulting knowledge might be of great use when interpreting the behavior of an SCM or GCM as a whole. These models are only too often treated as ''black boxes,'' by comparing results of different models without a good understanding of what causes the differences. By knowing the typical behavior of each closure method under certain conditions one might be able to recognize their fingerprint in the overall modeled state more easily.

The closures examined here are based on just two basic views on what controls the interaction at cloud base between the cloud layer and the subcloud layer. One considers the cloud-base mass flux to be entirely controlled by the dry convection in the subcloud layer. The clouds are seen as condensating thermals rooting deep in the subcloud layer, which at cloud base are thus controlled by nonlocal subcloud properties. The other view assumes that moist convective processes in the cloud layer dominate the cloud-base transport: latent heat release in the clouds drives the transport at cloud base. The cases of shallow cumulus studied here seem entirely dominated by subcloud turbulence, as shown by the good scaling of w_b^c with w_{sub}^*. In order to move further from domination by subcloud turbulence towards domination by cloud physics, it would be interesting to test for a diurnal cycle of deeper cumulus, for example, the case as used by GCSS Working Group IV for cloud-resolving model (CRM) and SCM intercomparison studies (Xu et al. 2002). This cloud reveal any limits of the closures based on subcloud domination.

Of the three closures studied here the moist static energy convergence closure produces the largest deviations from the cloud-base mass flux as diagnosed in LES. It can not deal with significant moisture and temperature tendencies in the subcloud layer, which leads to unrealistic intense vertical mixing resulting in a too rapidly deepening cloudy boundary layer when applied in the SCM. This might have serious implications. For example, a comparison of ECMWF model results to the measured hydrometeor occurrence at the ARM SGP site by Mace et al. (1998) showed that typically the model predicts the onset of deep cloud events too early. As deep (precipitating) convection in diurnal cycles is often preceded by shallow convection earlier in the day, it is likely that the development of the shallow cumulus cloud layer in time at least partially determines the onset of deep convection. A too rapidly deepening cloud layer caused by the moist static energy convergence closure might be one of the reasons for early triggering, as any capping inversion preventing deep convection is destroyed earlier.

The CAPE adjustment closure is based on the assumption that moist convective intensity immediately responds to convective instability as defined by CAPE, through the process of compensating subsidence. The evaluation shows that this closure predicts the wrong trend in the mass flux in the early and final stages of the existence of the cloud layer, when cloud-base transport is controlled by subcloud-layer processes. To work well, this closure needs a cloud layer of considerable depth on top of a well-developed dry convective layer driven by surface energy fluxes, a situation in which compensating subsidence might indeed dominate the breakdown of CAPE. Its use lies therefore more in the parameterization of deep convection, for which it was originally developed. Nevertheless studying the behavior of the CAPE closure in a diurnal cycle of shallow cumulus has been useful, as it reveals the possible consequences in situations of deep cumulus that are close to a transition from/to shallow cumulus, or are in the beginning/ending stages of the diurnal cycle.

For a diurnal cycle of shallow cumulus, the coupling of the mass flux activity at cloud base to the subcloud turbulent velocity scale clearly gives the best results, mainly because the development of the cloud core vertical velocity is neatly captured by w_{sub}^*. As a consequence the development of the thermodynamic structure of the boundary layer in RACMO SCM strongly resembles that in LES. By retaining the core fraction at cloud base in the formulation the closure knows when the dry subcloud-layer thermals reach their lifting condensation level, which gives a more smooth development of the cloud-base mass flux. Why the scaling of w_b^c with w_{sub}^* works better for the SCMS case than for the ARM case is another unresolved issue. The question is if the strict relation between subcloud TKE and vertical velocity at cloud base still holds for high-shear conditions, or significantly deeper cloud layers, where the cloud dynamics is expected to play a more significant role in the cloud–subcloud interaction. To that purpose other relevant scales can be included in the parameterization of the cloud-base vertical velocity, such as u^* and w_{cloud}^*. The formulation and evaluation of this concept is a subject for further research.

The results have raised some new questions. First, the mass flux closures have only been evaluated for a single diurnal cycle. The SCM results show that the impact of the mass flux closure on the development of the boundary layer can be significant. It is therefore interesting to know what the impacts will be on longer time scales. Second, how do different mass flux closures affect the spatial distribution of type and depth of moist convection? Jakob and Siebesma (2003) have already shown that the subcloud-layer model and the definition of the trigger function for moist convection have a significant impact on the ECMWF model state. Third, in the shallow cumulus cases studied here the large-scale

Unauthenticated | Downloaded 05/30/24 05:45 AM UTC

forcings were prescribed, and small compared to the energy input by the surface fluxes. One wonders what happens when the SCM is fully coupled to the large-scale dynamics, allowing for interactions between small (unresolved) and large (resolved) scales. For these reasons, a logical next step is to repeat the same evaluation but now with the closures implemented in a three-dimensional model, with full coupling to the large-scale dynamics. This should give insight into the impact of the closures on the convective cloud climatology on longer time scales, on the general circulation, and on the radiative budget. An example is the EUROCS intercomparison project on the Hadley cycle in the Northern Pacific, which is a semi-Lagrangian evaluation of single-column models along the trade wind flow in the lower troposphere.

Acknowledgments. The first author was affiliated at the Royal Netherlands Meteorological Institute (KNMI) when working on this paper. We thank the ARM SGP Data Archive for providing the observational data shown in Fig. 1. The LES results in this study were obtained using the supercomputer facilities of the European Centre for Medium-Range Weather Forecasts (ECMWF) in Reading, United Kingdom. This study has been supported by the European Project for Cloud Systems Studies (EUROCS), and by the Netherlands Organization for Scientific Research (NWO) under Grant 750.198.06. We thank two reviewers for critically reading this paper and for their useful remarks and suggestions.

APPENDIX

The RACMO SCM

a. Model description

A description of the RACMO SCM is given by Lenderink and Siebesma (2000). The model consists of a dry turbulence scheme for mixed-layer transport using a TKE mixing length (Lenderink and Holtslag 2004, manuscript submitted to *Quart. J. Roy. Meteor. Soc.*), a mass flux convection scheme for cloud-layer transport based on that of Tiedtke (1989), and a statistical cloud scheme based on the method of Cuijpers and Bechtold (1995). First, the heights of cloud base and cloud top are determined by lifting a parcel of surface air dry/moist adiabatically. Its lifting condensation level is cloud base, and above that its first level of negative buoyancy is cloud top. After the parcel ascent the dry turbulence scheme is executed for mixed-layer transport, distributing the surface sensible and latent heat fluxes over the mixed layer. For more detailed descriptions of the turbulence scheme see Lenderink and Holtslag (2003, manuscript submitted to *Quart. J. Roy. Meteor. Soc.*) or Lenderink and Siebesma (2000).

Next the closure for the cloud-base mass flux is carried out, after which the mass flux profile is calculated in the convection scheme. In the mixed layer, the mass flux is set to increase linearly with height toward its cloud-base value. In the cloud layer the fixed entrainment and detrainment rates $\epsilon = 2 \times 10^{-3}\ \mathrm{m}^{-1}$ and $\delta = 2.7 \times 10^{-3}\ \mathrm{m}^{-1}$ are used as suggested by Siebesma and Cuijpers (1995), found to be appropriate in SCM context by Siebesma and Holtslag (1996). Above cloud top a massive detrainment layer is situated to mimic the effects of cumulus overshoots into the capping inversion. It has a fixed depth of 2000 Pa, in which any remaining mass flux decreases exponentially.

For the cloud fraction the RACMO SCM in this study uses the method of Cuijpers and Bechtold (1995), in which the cloud fraction N_{CB95} is a function of the normalized saturation deficit Q_1,

$$N_{\mathrm{CB95}} = 0.5 + 0.36 \arctan(1.55 Q_1). \tag{A1}$$

For simplicity Q_1 is only a function of q_t,

$$Q_1 \equiv \frac{q_t - q_{\mathrm{sat}}}{\sigma_{q_t}}, \tag{A2}$$

where $\sigma^2_{q_t}$ is the variance of q_t. The variable σ_{q_t} needs to be parameterized, for which in RACMO SCM a simplified diagnostic budget equation is used as proposed by Lenderink and Siebesma (2000):

$$\overline{w' q_t'} \frac{\partial q_t}{\partial z} = \frac{\sigma^2_{q_t}}{\tau}.$$

This equation balances production of variance (left-hand side) and dissipation closed by a linear damping (right-hand side). Here τ is a time scale associated with the updrafts in the cumulus clouds:

$$\tau = l_{\mathrm{cloud}} / w^{\mathrm{cu}}_*,$$

with l_{cloud} the cloud depth and w^{cu}_* a moist convective vertical velocity scale (Grant and Brown 1999),

$$(w^{\mathrm{cu}}_*)^3 = \int_{\mathrm{cloud}} \frac{g}{\theta} M \Delta\theta_v \, dz. \tag{A3}$$

Here, $\Delta\theta_v$ is the virtual potential temperature excess of the bulk cumulus updraft, for which the rising parcel ascent is used as discussed earlier. As mass flux schemes have proven more successful than diffusion schemes to represent the turbulent fluxes for shallow cumulus, a mass flux approximation is used in the production term, which gives

$$M(q^u_t - \overline{q_t}) \frac{\partial q_t}{\partial z} \simeq \frac{w^{\mathrm{cu}}_*}{l_{\mathrm{cloud}}} \sigma^2_{q_t},$$

where q^u_t is the specific humidity of the bulk updraft. This equation expresses the balance between production on the large cumulus convective scale and dissipation on the small turbulent scales. We now arrive at the following expression for the variance,

$$\sigma^2_{q_t} \simeq \frac{M(q^u_t - \overline{q_t}) l_{\mathrm{cloud}}}{w^{\mathrm{cu}}_*} \frac{\partial q_t}{\partial z}.$$

Unauthenticated | Downloaded 05/30/24 05:45 AM UTC

Lenderink and Siebesma (2000) have shown that this method gives a reasonable σ_{q_t} for the ARM and BOMEX cases.

The simulations are carried out on a vertical grid of 40 levels covering the lowest 4 km of the atmosphere, which results in about 7 levels in the cloud layer. The time-integration step Δt is 60 s, which is small compared to the diurnal time scale. The surface fluxes as well as the large-scale forcings and initial conditions were prescribed, according to the setup of the LES cases as presented in section 3.

b. Closure implementation

The boundary layer quasi-equilibrium closure (7) is completely diagnostic, as all its variables are available at time t at the point of its calculation in the model hierarchy. Cloud-based height z_b is obtained by releasing a dry adiabatically rising parcel of surface air and calculating its lifting condensation level. The h flux at cloud base is estimated by integrating with height all tendencies in the subcloud layer; see Eq. (7). The result is the surface flux plus forcings minus the small flux of the still active turbulence scheme at cloud base.

The CAPE adjustment closure (13) needs the θ_v^p profile of a moist adiabatically rising parcel of near-surface air, and the profile of the normalized mass flux m. We follow Nordeng (1994) by using the values of the right-hand side variables in (13) at time $t - \Delta t$ to calculate M_b^c at time t. If no shallow convection occurred at the previous time step, a small minimum value of 0.01 m s^{-1} is assumed for M_b^c.

The closure (17) only needs w^*_{sub}, which can easily be calculated from the surface buoyancy flux $\overline{w'\theta'_v}^s$ and the mixed-layer height z_b. Version (19) needs the cloud fraction $N_{\text{CB}}95$ at cloud base, for which we use its value at time $t - \Delta t$.

REFERENCES

Arakawa, A., and W. H. Schubert, 1974: Interaction of a cumulus cloud ensemble with the large-scale environment, Part I. *J. Atmos. Sci.,* **31,** 674–701.

Augstein, E., H. Riehl, F. Ostapoff, and V. Wagner, 1973: Mass and energy transports in an undisturbed Atlantic trade-wind flow. *Mon. Wea. Rev.,* **101,** 101–111.

Betts, A. K., 1973: Non-precipitating cumulus convection and its parameterization. *Quart. J. Roy. Meteor. Soc.,* **99,** 178–196.

——, 1976: Modeling subcloud layer structure and interaction with a shallow cumulus layer. *J. Atmos. Sci.,* **33,** 2363–2382.

——, 1986: A new convective adjustment scheme. Part I: Observational and theoretical basis. *Quart. J. Roy. Meteor. Soc.,* **112,** 677–691.

——, 1997: The parameterization of deep convection. *The Physics and Parameterization of Moist Atmospheric Convection,* R. K. Smith, Ed., NATO ASI Series C, Vol. 505, Kluwer Academic, 255–279.

——, and M. J. Miller, 1986: A new convective adjustment scheme. Part II: Single column tests using GATE wave, BOMEX, ATEX and arctic air-mass data sets. *Quart. J. Roy. Meteor. Soc.,* **112,** 693–709.

——, and C. Jakob, 2002: Study of diurnal cycle of convective precipitation over Amazonia using a single column model. *J. Geophys. Res.,* **107,** 4732, doi: 10.1029/2002JD002264.

Brown, A. R., and Coauthors, 2002: Large-eddy simulation of the diurnal cycle of shallow cumulus convection over land. *Quart. J. Roy. Meteor. Soc.,* **128,** 1075–1093.

Browning, K. A., 1993: The GEWEX Cloud System Study (GCSS). *Bull. Amer. Meteor. Soc.,* **74,** 387–399.

Cuijpers, J. W. M., and P. Bechtold, 1995: A simple parameterization of cloud water related variables for use in boundary layer models. *J. Atmos. Sci.,* **52,** 2486–2490.

Deardorff, J. W., 1970: Convective velocity and temperature scales for the unstable planetary boundary layer and for Rayleigh convection. *J. Atmos. Sci.,* **27,** 1211–1212.

Emanuel, K. A., 1994: *Atmospheric Convection.* Oxford University Press, 580 pp.

Esbensen, S., 1975: An analysis of subcloud-layer heat and moisture budgets in the western Pacific trades. *J. Atmos. Sci.,* **32,** 1921–1923.

——, 1978: Bulk thermodynamic effects and properties of small tropical cumuli. *J. Atmos. Sci.,* **35,** 826–837.

Fritsch, J. M., and C. F. Chappell, 1980: Numerical prediction of convectively driven mesoscale pressure systems. Part I: Convective parameterization. *J. Atmos. Sci.,* **37,** 1722–1733.

Grant, A. L. M., 2001: Cloud-base fluxes in the cumulus-capped boundary layer. *Quart. J. Roy. Meteor. Soc.,* **127,** 407–422.

——, and A. R. Brown, 1999: A similarity hypothesis for shallow cumulus transports. *Quart. J. Roy. Meteor. Soc.,* **125,** 1913–1936.

Gregory, D., J.-J. Morcrette, C. Jakob, A. C. M. Beljaars, and T. Stockdale, 2000: Revision of convection, radiation and cloud schemes in the ECMWF Integrated Forecasting System. *Quart. J. Roy. Meteor. Soc.,* **126,** 1685–1710.

Holland, J. Z., and E. M. Rasmusson, 1973: Measurements of the atmospheric mass, energy, and momentum budgets over a 500-kilometer square of tropical ocean. *Mon. Wea. Rev.,* **101,** 44–55.

Jakob, C., and A. P. Siebesman, 2003: A new subcloud model for mass-flux convection schemes: Influence on triggering, updraft properties, and model climate. *Mon. Wea. Rev.,* **131,** 2765–2778.

Kuo, H. L., 1965: On formation and intensification of tropical cyclones through latent heat release by cumulus convection. *J. Atmos. Sci.,* **22,** 40–63.

——, 1974: Further studies of the parameterization of the influence of cumulus convection on large-scale flow. *J. Atmos. Sci.,* **31,** 1232–1240.

LeMone, M. A., and W. T. Pennell, 1976: The relationship of trade wind cumulus distribution to subcloud layer fluxes and structure. *Mon. Wea. Rev.,* **104,** 524–539.

Lenderink, G., and A. P. Siebesma, 2000: Combining the mass flux approach with a statistical cloud scheme. Preprints, *14th Symp. on Boundary Layer and Turbulence,* Aspen, CO, Amer. Meteor. Soc., CD-ROM, 2.9.

Mace, G. G., C. Jakob, and K. P. Moran, 1998: Validation of hydrometeor occurrence predicted by the ECMWF model using millimeter wave radar data. *Geophys. Res. Lett.,* **25,** 1645–1648.

Manabe, S., J. Smagorinsky, and R. F. Stricker, 1965: Simulated climatology of a general circulation model with a hydrologic cycle. *Mon. Wea. Rev.,* **93,** 769–798.

Moeng, C.-H., and P. P. Sullivan, 1994: A comparison of shear- and buoyancy-driven planetary boundary layer flows. *J. Atmos. Sci.,* **51,** 999–1022.

Neggers, R. A. J., 2002: Shallow cumulus convection. Ph.D. thesis, Wageningen University, 202 pp.

——, P. G. Duynkerke, and S. M. A. Rodts, 2003: Shallow cumulus convection: Validation of large-eddy simulation against aircraft and LandSat observations. *Quart. J. Roy. Meteor. Soc.,* **129,** 2671–2696.

Nitta, T., and S. Esbensen, 1974: Heat and moisture budget analyses using BOMEX data. *Mon. Wea. Rev.,* **102,** 17–28.

Nordeng, T. E., 1994: Extended versions of the convective parame-

Unauthenticated | Downloaded 05/30/24 05:45 AM UTC

trization scheme at ECMWF and their impact on the mean and transient activity of the model in the tropics. Tech. Memo. 206, ECMWF, Shinfield Park, Reading, United Kingdom, 41 pp.

Ogura, Y., and H.-R. Cho, 1974: On the interaction between the subcloud and cloud layers in tropical regions. *J. Atmos. Sci.*, **31,** 1850–1859.

Ooyama, K., 1971: A theory on parameterization of cumulus convection. *J. Meteor. Soc. Japan,* **49,** 744–756.

Randall, D. A., D.-M. Pan, P. Ding, and D. G. Cripe, 1997: Quasi-equilibrium. *The Physics and Parameterization of Moist Atmospheric Convection*, R. K. Smith, Ed., NATO ASI Series C, Vol. 505, Kluwer Academic, 359–385.

Raymond, D. J., 1995: Regulation of moist convection over the west Pacific warm pool. *J. Atmos. Sci.,* **52,** 3945–3959.

Siebesma, A. P., and J. W. M. Cuijpers, 1995: Evaluation of parametric assumptions for shallow cumulus convection. *J. Atmos. Sci.,* **52,** 650–666.

——, and A. A. M. Holtslag, 1996: Model impacts of entrainment and detrainment rates in shallow cumulus convection. *J. Atmos. Sci.,* **53,** 2354–2364.

——, and Coauthors, 2003: A large eddy simulation intercomparison study of shallow cumulus convection. *J. Atmos. Sci.,* **60,** 1201–1219.

Stokes, G. M., and S. E. Schwartz, 1994: The Atmospheric Radiation Measurement (ARM) Program: Programmatic background and design of the cloud and radiation test bed. *Bull. Amer. Meteor. Soc.,* **75,** 1201–1222.

Tiedtke, M., 1989: A comprehensive mass flux scheme for cumulus parameterization in large-scale models. *Mon. Wea. Rev.,* **117,** 1779–1800.

White, P. W., Ed., 2001: Physical processes. Integrated Forecasting System (IFS) documentation, Cycle CY23r4, ECMWF, 166 pp. [Available online at http://www.ecmwf.int/research/ifsdocs/.]

Xu, K.-M., and Coauthors, 2002: An intercomparison of cloud-resolving models with the Atmospheric Radiation Measurement summer 1997 Intensive Observation Period data. *Quart. J. Roy. Meteor. Soc.,* **128,** 593–624.

Unauthenticated | Downloaded 05/30/24 05:45 AM UTC